Processing and in vitro bioactivity of high-strength 45S5 glass-ceramic scaffolds for bone regeneration

Aguilar-Reyes, Ena A.; León-Patiño, Carlos A.; Villicaña-Molina, Esmeralda; Macías-Andrés, Víctor I.; Lefebvre, Louis-Philippe

Publisher's version / Version de l'éditeur:
https://doi.org/10.1016/j.ceramint.2017.02.107
Ceramics International, 43, 9, pp. 6868-6875, 2017-06

Ceramics International xxx (xxxx) xxx–xxx

Contents lists available at ScienceDirect

Ceramics International

journal homepage: www.elsevier.com/locate/ceramint

Processing and in vitro bioactivity of high-strength 45S5 glass-ceramic scaffolds for bone regeneration

Ena A. Aguilar-Reyes[a,*], Carlos A. León-Patiño[a], Esmeralda Villicaña-Molina[a], Víctor I. Macías-Andrés[a], Louis-Philippe Lefebvre[b]

[a] Instituto de Investigación en Metalurgia y Materiales, Universidad Michoacana de San Nicolás de Hidalgo, Edif. U, Av. Francisco J. Múgica S/N Ciudad Universitaria, C.P. 58030 Morelia, Michoacán, México

[b] National Research Council Canada (NRC), Boucherville Research Facilities, 75 de Mortagne Boulevard, Building BOU-1, Boucherville, Quebec, Canada J4B 6Y4

ARTICLE INFO

Keywords:
A. Sintering
B. Porosity
C. Strength
D. Glass ceramics
E. Biomedical applications

ABSTRACT

In this paper, the compressive strength and in vitro bioactivity of sintered 45S5 bioactive glass scaffolds produced by powder technology and polymer foaming were investigated. The sintering temperature of scaffolds was 975 °C. The characterization of scaffolds before immersion in SBF was performed by scanning electron microscopy (SEM) and microtomography (μCT). The scaffolds were also tested for compression, and their density and porosity were measured. After immersion, the samples were observed through SEM and analyzed using EDS, X-ray diffraction (XRD), and infrared spectroscopy (FT-IR). Mass variation was also estimated. The glass-ceramic scaffolds showed a 61.44 ± 3.13% interconnected porosity and an average compressive strength of 13.78 ± 2.43 MPa. They also showed the formation of a hydroxyapatite layer after seven days of immersion in SBF, demonstrating that partial crystallization during sintering did not suppress their bioactivity.

1. Introduction

The potential of bioceramic materials for tissue regeneration has been shown in vitro and in clinical practice. Certain bioactive glasses that have the ability to regenerate both soft and hard tissues are composed of these materials. The bioactivity of a material has been associated with the formation of hydroxyapatite crystals on the surface that is in contact with natural or simulated body fluid (SBF), similar to the inorganic structure of bone. In addition, bioactive glasses have been shown to exert control over the production of osteoblasts in the cell cycle [1]. This discovery has stimulated research on the use of bioactive glasses as scaffolds for tissue engineering. It has been demonstrated that bioactive glass 45S5, also known as Bioglass®, has the greatest potential to be used as a three-dimensional matrix (regenerative scaffold) in a large number of human bone components; although it crystallizes during sintering, its bioactivity slows down but it is not eliminated [2–4]. Recent studies have shown that the ability to regenerate human tissue through the formation of a hydroxyapatite surface layer depends on the porosity of the 3D bioactive glass structure, given that the scaffold has greater capacity when it is more porous [5–8]. Note that this porosity should be interconnected with proper pore size (300–500 μm) to enable cell infiltration, tissue ingrowth and vascularization, and nutrient delivery to the center of the regenerated tissue [7]. For these reasons, research continues to study the different ways of producing Bioglass® foams with characteristics similar to those of human bone. Currently, three methods are used to produce porous foams: the replica technique, the sacrificial template technique, and the direct foaming technique [9]. In the replica technique, a polymeric sponge (e.g. a polyurethane foam) is initially dip coated in a glass powder suspension, followed by oven drying and burning out of the polymer template. Finally, the glass or glass-ceramic structure is densified through sintering at high temperatures. The sacrificial template method involves the preparation of a composite made up of a sacrificial phase mixed with glass particles. The sacrificial phase is extracted (usually thermally) from the partially consolidated matrix to generate pores within the microstructure. This method leads to porous materials that display a negative replica of the original sacrificial template, as opposed to the positive morphology obtained from the replica technique described above. In the direct foaming method, a gas is incorporated into a glass or ceramic slurry to produce a foam, typically by bubbling air or an inert gas through the slurry.

The main objective of the present study was to implement a methodology to obtain bioactive scaffolds from Bioglass® powders and to examine the relationships between their microstructure and

* Corresponding author. Present/permanent address: Instituto de Investigación en Metalurgia y Materiales, Universidad Michoacana de San Nicolás de Hidalgo, Edif. U, Av. Francisco J. Múgica S/N Ciudad Universitaria, C.P. 58030 Morelia, Michoacán, México.
E-mail address: aareyes@umich.mx (E.A. Aguilar-Reyes).

http://dx.doi.org/10.1016/j.ceramint.2017.02.107
Received 1 June 2016; Received in revised form 20 February 2017; Accepted 22 February 2017

bioactivity. The combined method of powder technology and polymer foaming control the porosity, pore size, and compression strength of the scaffolds by varying the ratio of the foaming agent/binder/Bioglass® powder and the sintering temperature. This work was based on the principle that it is possible to obtain controlled re-absorption and dissolution rates of species that promote tissue regeneration through the production of glasses with a structure that mimics that of trabecular bone. The in vitro bioactivity of the Bioglass® scaffolds was monitored by evaluating the formation of the calcium phosphate layer on their surfaces after soaking in SBF.

2. Materials and methods

2.1. Preparation of the 45S5 bioactive glass

The 45S5 bioactive glass was obtained through the traditional melting-quenching technique of a mixture of high-purity SiO_2, Na_2CO_3, CaO, and P_2O_5 (Sigma-Aldrich, St. Louis, MO, USA) powders that were stoichiometrically prepared to produce the final composition of 24.5Na2O-24.5CaO-6P2O5-45SiO_2 (wt%). After being dry-mixed in a conventional ball mill for 30 min, the powder was placed in a fused silica crucible and heated to an intermediate step at 900 °C for 90 min to degasify the melt, followed by a second step at 1350 °C for 90 min in a Carbolite HTF 17/10 Furnace. The melt was then quenched in air on a stainless steel plate. Next, the glass was dry-ground in a Siebtechnik T750 Laboratory Disc Mill for 1 min and sieved to obtain fine powders with a particle size smaller than 63 μm (d_{10}=2.7 μm; d_{50}=21.9 μm and d_{90}=61 μm), as determined by the light scattering technique (Beckman Coulter LS 13 320; Beckman Coulter, Brea, CA, Fraunhofer optical model).

2.2. Fabrication of 45S5 Bioglass® glass scaffolds

The 45S5 bioactive glass scaffolds were produced through the combination of powder technology and the polymer foaming method [10]. The glass powder was dry-mixed with a solid polymeric binder (Varcum 29217, Durez Corporation, Niagara Falls, NY, USA) and a foaming agent (p-toluenesulfonyl hydrazide or TSH, Sigma-Aldrich, St. Louis, MO, USA) at a ratio of 45/54.5/0.5 in wt%, respectively. The mixing of the powders was performed for 45 min in a Shake-Mixer Glen Mills WAB, Model T-F2, using a glass container and 10-mm-diameter stainless steel balls. The powder mixture was then poured into an alumina mold (3 cm in diameter, 5 cm in height and 5 mm in thickness) for foaming. The foaming was carried out in a Thermolyne FB1300 Muffle Furnace. Afterwards, the foams were rectified into small cylinders of 10–18 mm in diameter and 20–30 mm in length, followed by the debinding and sintering steps, which were done in a Carbolite HTF 17/10 Furnace.

2.3. Bioactivity tests

The cylindrical scaffolds were cut into discs with dimensions of 10 mm in diameter and 3 mm in thickness. Prior to the bioactivity tests, the discs were sterilized in an ultrasonic bath with ethanol and acetone for 30 min. Next, they were dried in an oven for 24 h and exposed to ultraviolet irradiation for 40 min. Various times were selected for immersion in SBF: 1, 3, 7, 14, 21, and 28 days, using three samples for each immersion time. Each disc was immersed in 17.5 ml of acellular simulated body fluid (SBF), following the protocol published by Kokubo et al. [11]. The immersed discs were maintained at 37 °C in polyethylene vials under sterile conditions in a cell culture room. After soaking for different periods in the SBF, the specimen was taken out of the SBF and gently washed with pure water. The specimen was dried in an oven at 90 °C for 24 h and subsequently placed in a desiccator.

2.4. Characterization of the 45S5 bioactive glass scaffolds

The microstructure of the scaffolds was characterized using a JSM-6100 JEOL scanning electron microscope (JEOL, Tokyo, Japan) and an X-Tek HMXST 225 X-ray μCT (Nikon Metrology, Tring, UK). Before and after the bioactivity tests, the scaffolds were characterized by X-ray diffraction (Bruker AXS D8 Discover X-Ray Diffractometer) to determine the crystalline phases after sintering and the evolution of the hydroxyapatite layer, respectively. The acquisition data were obtained in the range of 20–90° in 2θ, using CuKα (λ=0.15405 nm) radiation as the source, with a 0.04° step and 2 s/step. Functional groups of bioactive glass and hydroxyapatite phases were determined in the 45S5 bioactive glass scaffolds through infrared spectroscopy, before and after immersion in SBF. Each spectrum was comprised of 32 independent scans in transmittance, measured at a spectral resolution of 1 cm^{-1} within the 4000–400 cm^{-1} range, in a Bruker Tensor 27 FT-IR Spectrometer (Bruker, Germany).

For unconfined compression tests, experiments were conducted using a minimum of 10 randomly selected scaffolds (10 mm in diameter and 5–9 mm in height), which were tested in a universal MTS machine with a cell load of 5 kN. The cross-head loading speed was set at 2.5 mm/min.

The density of the foams was calculated using the mass and dimensions (diameter and height) of the sintered cylinders. The average density was calculated from 40 samples.

3. Results and discussion

The final scaffold had a low-density, open-cell structure. The average density calculated from their dimensions and weight was 1.04 ± 0.08 g/cm^3. The porosity was 61.44 ± 3.13%, and the volume decreased by approximately 25% of the initial volume, after debinding and sintering (Fig. 1). After foaming, the cylindrical foams were

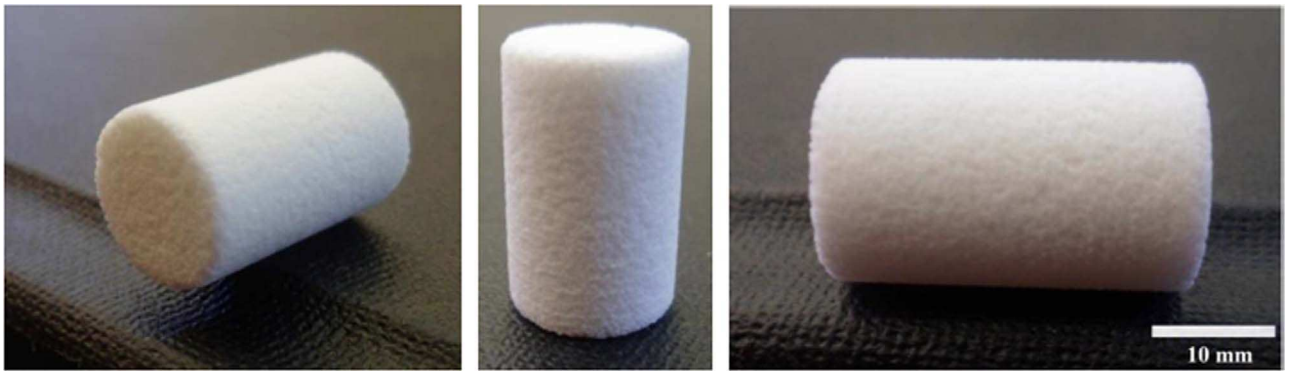

Fig. 1. 45S5 bioactive glass-ceramic scaffolds produced by the powder technology approach.

rectified to a diameter of 18 mm. During the debinding and sintering steps, the foam underwent shrinkage up to a diameter of 10 mm. According to Bretcanu et al. [12], two distinct sintering steps can be distinguished in the heat treatment of 45S5 Bioglass®: a first stage and a longer and more marked stage. The first densification step starts at 500 °C and ends at 600 °C. The second densification step starts at 950 °C. The first step of densification occurs shortly after the glass transition temperature is reached. The Bioglass® particles crystallize in the range of 600–750 °C, depending on the heating rate. The second densification step is set between the crystallization and melting temperatures. Thus, the material is highly crystalline prior to undergoing the second step of densification (above 850 °C). The shrinkage associated with the first step is around 12%, whereas samples are found to shrink more during the second densification step (around 36%). The results obtained in the present work are in agreement with these findings.

The porous material in the present work was produced from a dry powder mixture composed of a bioactive glass powder, an organic solid binder, and a foaming agent. During the foaming step, the binder was melted at 55 °C to form a suspension with the glass particles and foaming agent. The foaming agent then decomposed (105–110 °C) to generate and release the gas (mainly N_2 and CO_2) that expanded the structure and created the interconnected porosity. The solid foamed structures comprising the Bioglass® particles embedded in the polymer binder were then heated at 500 °C for 2 h to burn out the binder. Finally, the sintering was performed in air at 975 °C for 1 h to create interparticle bonds and to consolidate the remaining inorganic tridimensional network into a rigid structure with interconnected porosity, thus providing the foam with its physical and mechanical properties and simultaneously crystallizing the glass. Sintering conditions (tem-

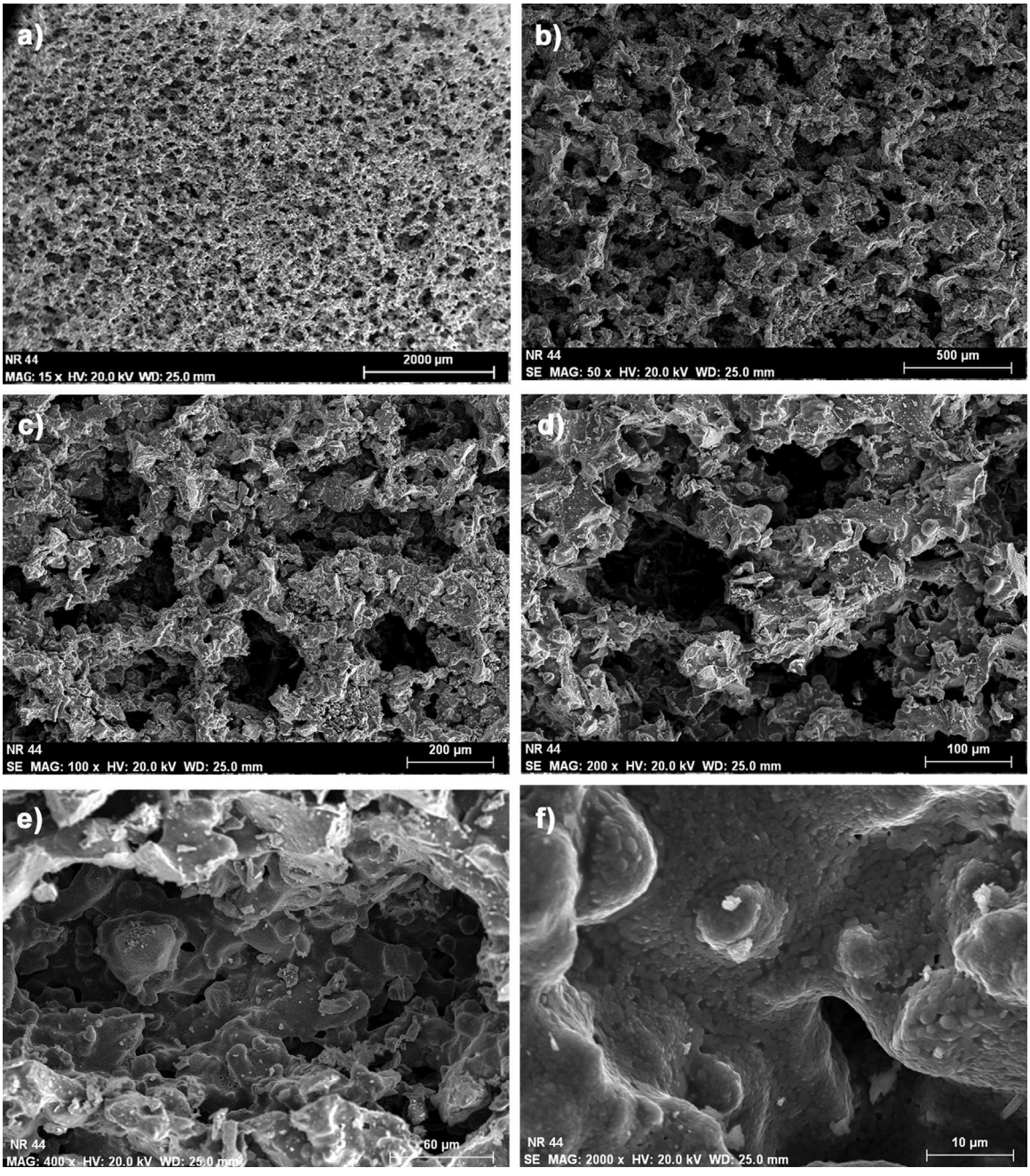

Fig. 2. SEM images of porous structure of 45S5 bioactive glass scaffolds sintered at 975 °C at various magnifications: (a) 15×, (b) 50×, (c) 100×, (d) 200×, (e) 400× and (f) 2000×. Note the presence of micropores within the single large pore.

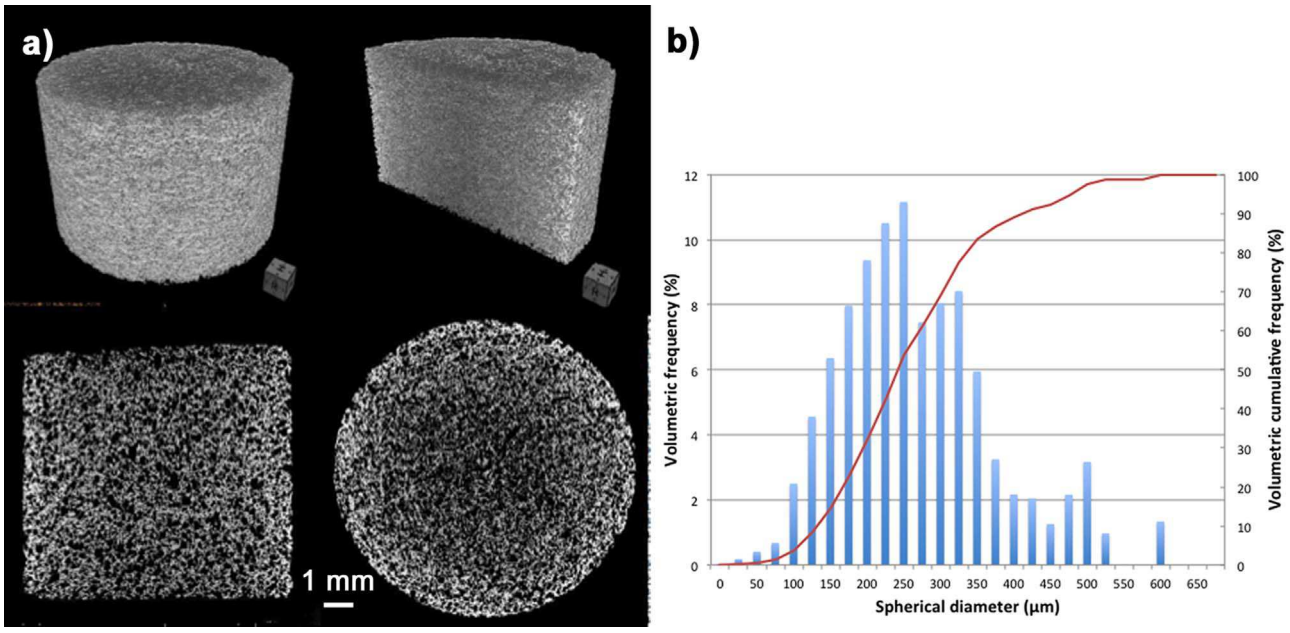

Fig. 3. (a) Pore size distribution and (b) microtomography (μCT) of a 45S5 bioactive glass scaffold sintered at 975 °C.

perature, time, and atmosphere) must be such that interparticle bonds are created, while extensive densification is avoided. Sintering temperature greatly depends on the material. To avoid densification, the material is typically sintered at temperatures ranging from 30% to 90% of the melting temperature of the material. In this work, 975 °C was equal to 85% of the melting temperature of the 45S5 bioactive glass (1145 °C). The resulting scaffolds have three different levels of porosity that are dependent on the three-stage powder technology and the polymer foaming approach. Large porosity may be attributed to the formation of the cells and their coalescence during foaming, and intermediate porosity to the windows formed in the cell wall during foaming and to the decomposition of the binder during debinding, as well as to the fine microporosity between the particles. Open-cell foams have a reticular structure. During foaming, the bulk material concentrates entirely on the cell sides, shaping the struts. Thus, the solid matrix is composed of struts oriented in different directions in space and whose thickness is always much smaller than the cell diameter. Depending on sintering temperature and duration, the fine microporosity may be reduced during sintering, and the mechanical strength may be adjusted for application. Fine particles, low binder content, and high sintering temperature provide greater mechanical strength. The SEM images at various magnifications of the sintered scaffolds in Fig. 2 show a uniform porous structure throughout the sample and the interconnection of the intermediate and large porosities with a pore size in the range of 25–600 μm. At higher magnifications, the microporosity between the sintered glass particles in the walls and struts is clearly observed.

Fig. 3(a) shows 2-D and 3-D microtomography (μCT) images obtained from the sintered scaffolds. A uniform and interconnected porosity, as well as the thickness of the struts in the scaffolds, can be observed. The graph in Fig. 3(b) depicts the pore size distribution: the volumetric frequency up to 10.5% for a pore size of 250 μm is on the left axis, and the volumetric cumulative frequency up to 100% is on the right axis. The scaffolds exhibited a wide pore size distribution ranging

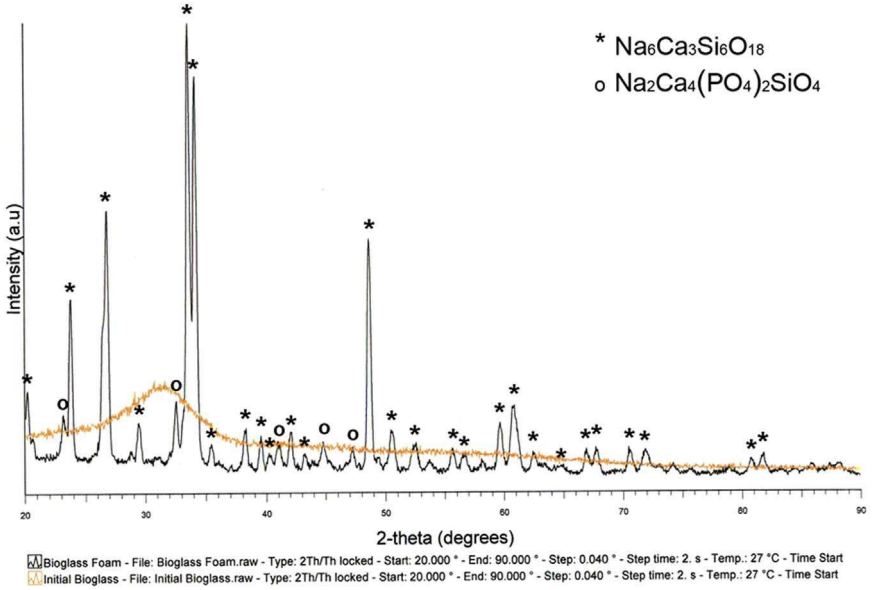

Fig. 4. XRD spectra of 45S5 Bioglass powder and Bioglass scaffold sintered at 975 °C.

from 25 to 600 μm, preferentially in the size class (100–400 μm) that is within the range of the required parameters (50–600 μm) for regenerative scaffolds [13,14],

Fig. 4 shows the XRD patterns of the 45S5 bioactive glass and foams sintered at 975 °C. The spectrum of the powder shows that the initial powder for producing foams is amorphous. However, the foam spectrum shows peaks representative of the crystalline phases: $Na_6Ca_3Si_6O_{18}$ (associated with $Na_2CaSi_2O_6$ JCPDS-ICDD 01-077–2189) and $Na_2Ca_4(PO_4)_2SiO_4$ (JCPDS-ICDD 29-1193). The same has been identified by other researchers in previous studies of sintered bioactive glasses of the same composition [11,15–17]. This clearly indicates that a process of crystallization is present during the sintering of foams.

The specific surface area, which is an important feature that influences aspects such as reaction kinetics, and that is required to calculate the SBF volume for immersion of each sample, was measured in a HORIBA-SA 9600 series surface area analyzer. The gas used for the analysis was nitrogen, and the obtained value for the Bioglass® scaffolds was 0.13 m^2/g.

The formation of the hydroxyapatite layer on the surface of the glass-ceramic scaffolds as a function of immersion time in SBF can be followed in Fig. 5. The initial clean surface of the sintered bioactive glass particles before immersion in SBF (Fig. 5(a)) can be observed, as well as how the hydroxyapatite tends to form agglomerates of spherical nanoparticles at seven days of immersion in SBF (Fig. 5(b)). The scaffold surfaces after 21 days of immersion in SBF are shown in Fig. 5(c) and, at higher magnification, in Fig. 5(d).

The presence of the hydroxyapatite phase was also confirmed by FT-IR analysis. The FTIR spectra of the 45S5 bioactive glass scaffold sintered at 975 °C, before and after immersion in SBF for 14 days, shown in Fig. 6, reveal the presence of characteristic peaks associated with the formation of the hydroxycarbonate apatite layer. The infrared spectra were plotted in the range of 1600–400 cm^{-1}, which is the region of special interest. According to Filho et al. [18], the 45S5 glass-ceramics with crystallinity up to 100% maintained their bioactivity when tested in SBF solution. Small peaks, the P-O vibrational band, which is indicative of a well-established amorphous calcium-phosphate layer at 965–960 cm^{-1} and at 600 cm^{-1}, appeared as an in vitro response of the 45S5 scaffolds soaked in SBF solution [16,18–22]. There are bands in the 1100–1000 cm^{-1} region, associated with the Si-O-Si stretching vibrational modes; 950–900 cm^{-1} related to the Si-O-non-bridging oxygen band (NBO); 770–720 cm^{-1}, which are associated with large surface 3D silica structures (Si-O-Si, Si-OH, or SiO^-); and 450–540 cm^{-1}, resulting from Si-O-Si bending. These bands become much sharper due to the crystallization process, and the absence of the Si-O-Si mode indicates a thick, well-established crystalline HCA layer [12,18,20]. As shown in Fig. 6, the abovementioned peaks decreased their intensity after immersion in SBF. The decrease in the non-bridging oxygen peak near 919 cm^{-1} reveals the release of Na^+ and Ca^{2+} into the solution [16]. Peaks associated with the crystal phase of the glass-ceramic emerged at 531 cm^{-1}, 578 cm^{-1}, and 622 cm^{-1}, which are attributed to the vibrational modes of P-O bending crystal [16,18]. The band at 579 cm^{-1}can be attributed to the silicorhenanite phase, as stated by Magallanes-Perdomo et al. [20]. Samples presented peaks at 1493 cm^{-1} and 1449 cm^{-1} related to the presence of carbonates. The carbonate peak detected at 1449 cm^{-1} can be absorbed atmospheric CO_2 and/or dissolved CO_2 [20]. The peak centered at approx. 880 cm^{-1} in the scaffold immersed in SBF is also attributed to C-O stretch vibrations (range 890–800 cm^{-1}) [19,22]. Therefore, this calcium silicate glass-ceramic scaffold exhibits in vitro bioactivity because of the presence of the HA phase. Thus, the next stage in preclinical trials would be to investigate its ability to sustain an

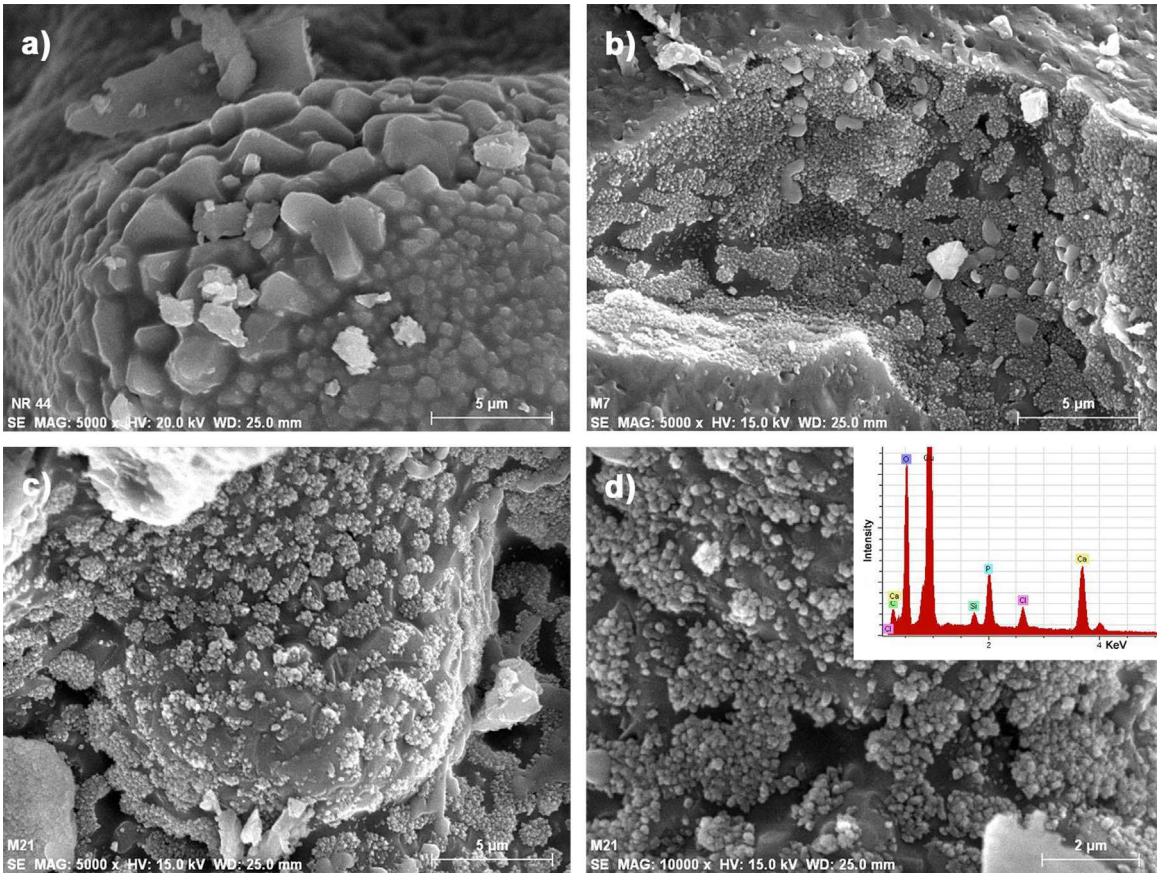

Fig. 5. SEM micrographs showing the development of the hydroxyapatite layer on the surface of bioactive glass-ceramic scaffolds at various immersion times in SBF: (a) 0, (b) 7, (c) and (d) 21 days.

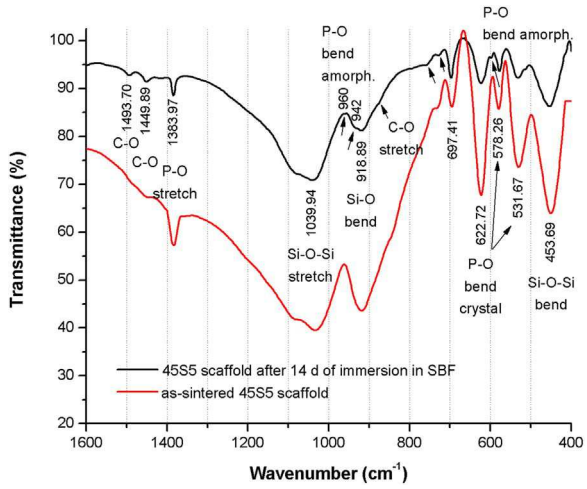

Fig. 6. FTIR of the 45S5 glass-ceramic scaffolds before and after immersion for 14 days in simulated body fluid.

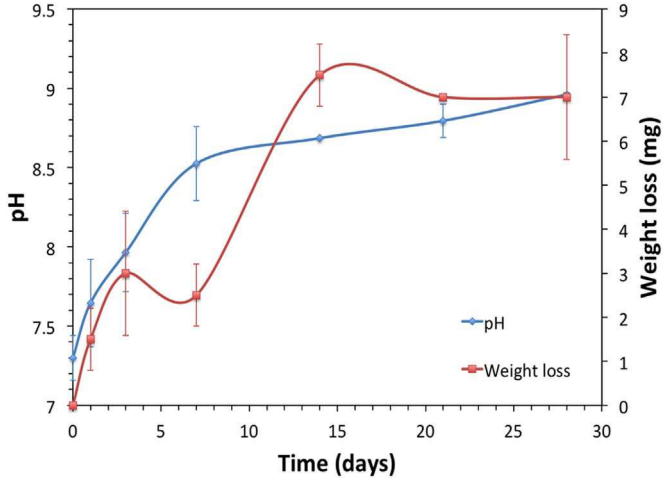

Fig. 7. The variation of pH in SBF immersion medium containing sintered scaffold and weight loss of sintered scaffold over time.

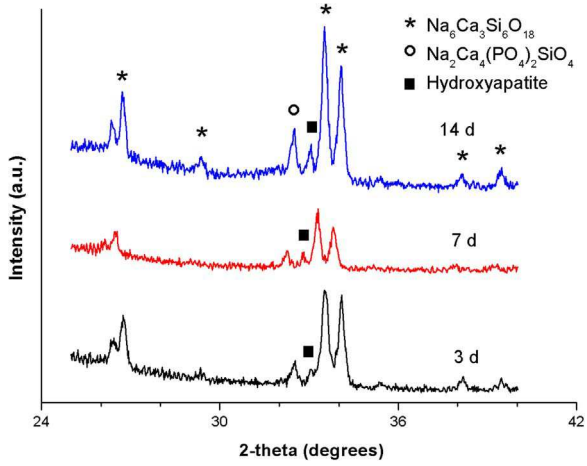

Fig. 8. XRD spectra of the as-sintered 45S5 scaffolds soaked in SBF for increasing times.

osteoblast cell culture.

Fig. 7 shows the pH variations as a function of the immersion time resulting from the solubility/ionic exchange reactions occurring at the solid/liquid interface. The pH of the SBF in which the scaffolds were immersed showed an initial increase, after which it remained relatively stable at a slightly alkaline pH of 9. This is to be expected, as more

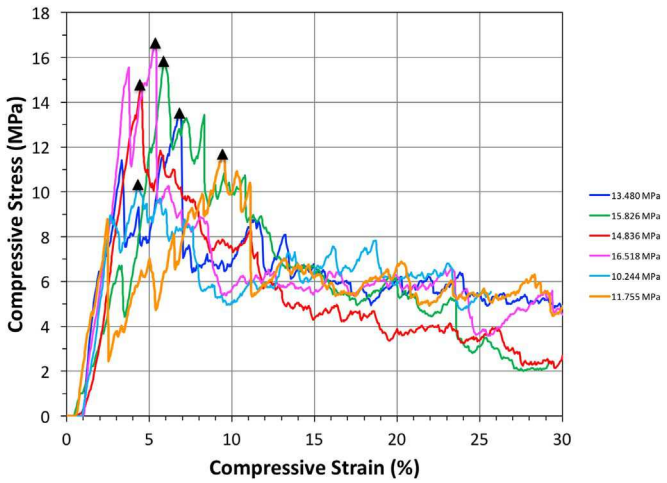

Fig. 9. A typical compressive stress-strain curve of the 45S5 bioactive glass foams sintered at 975 °C for 1 h.

sodium and calcium ions are released. During the first seven days of immersion in SBF, the pH of the 45S5 bioactive glass increased from 7.4 (the initial pH of the SBF solution) to 8.7, followed by gradual, smaller increments with increased immersion time. According to the mechanism proposed by Hench [23], the exchange of Na^+/H^+ ions is responsible for the increase in pH. On the other hand, the weight loss of glass-ceramic scaffolds over time was also registered and is plotted in Fig. 7. At the beginning, small variations were observed at up to seven days of immersion. Then, from 7 to 14 days, there was greater weight loss. Finally, weight loss remained constant at up to 28 days of immersion. It has been mentioned in the literature that 45S5 tends to crystallize during heat treatments due to the relatively low percentage of silica and the high content of network modifiers. Additionally, it has been noted that crystallization during sintering has adverse effects on the bioactivity of the scaffolds and can even suppress it [4]. However, as shown in the present results, crystallization only slowed down the bioactivity. As seen in Fig. 7, the variation in pH of the SBF in which the sintered 45S5 scaffolds were immersed was not pronounced in the early stage, compared with the 45S5 Bioglass® [24], in which more noticeable changes occurred in the earliest immersion period (the first 24 h of the experiment). When $Na_2Ca_2Si_3O_9$ phase is present, the $Na_2CaSi_2O_6$ crystalline phase, which is isostructural to $Na_2Ca_2Si_3O_9$ [15], is likely to undergo amorphization during immersion in a simulated physiological solution that preserves the bioactivity of the material [25]. In the present work, the HA layer was observed through SEM at seven days of immersion in SBF (Fig. 5), which indicates that the 45S5 scaffolds are still bioactive, even though crystallization had occurred during sintering. Fig. 8 shows the XRD spectra of the as-sintered scaffolds soaked in SBF for different periods, corroborating the presence of the HA layer. The first peak, corresponding to hydroxyapatite, can be seen at about $2\theta = 32 - 33°$, according to JCPDS-ICDD 01-084-1998.

Compression tests were carried out on scaffolds sintered at 975 °C. Typical stress-strain curves are presented in Fig. 9. Said curves are representative of those generally obtained with ceramic and glass scaffolds. They are highly corrugated due to their brittle nature and the successive fracture of the struts. The compressive strength of the scaffolds, defined as the maximum in the compression curves, was 13.78 ± 2.43 MPa, on average. This is a very high value compared with that of cancellous bone, which is reported to be in the range of 2–12 MPa [26]. The increase in compressive strength may be associated with the density of the materials obtained.

Regarding the properties of the 45S5 scaffolds produced, Table 1 summarizes the results obtained by various authors using several methods to manufacture the porous structures of bioactive materials for the same purpose as this research. The compressive strengths are

Table 1
Comparison of properties for scaffolds produced by various methods.

Ref.	Year	Technique	Material	Properties			
				Porosity (%)	Compression Strength (MPa)	Pore Size (μm)	Max. Bioactivity (days)
[27]	2000	Foaming of sol-gel systems	HA	76.7–80.2	4.7–7.4	20–1000	–
[28]	2002	Foaming of sol-gel systems	100S, 70S30C and 58S	–	–	100–200	–
[29]	2002	Replica (Polymer template)	HA	85–97	0.01–0.017	420–560	–
[30]	2002	Foaming of sol-gel systems	HA	76.7–80	1.6–5.8	100–500	–
[31]	2003	Gel-casting and polymer sponge methods	HA	70 77	0.55–5	200–400	–
[32]	2004	Gel-casting and polymer sponge methods	TCP+HA	73	9.8	200–400	–
[33]	2004	Foaming of sol-gel systems	Bioglass 70S30C	70–95	0.5–2.5	600	–
[34]	2004	Replica (Polymer template)	HA	69 y 86	0.8–1.2	490–1130	–
[35]	2005	Replica (Polymer template)	HA	85	0.2	420–560	–
[36]	2010	Replica (Polymer template)	PCL9 and Bioglass	60	0.8	100–150	–
[37]	2011	Gel-cast foaming process	Glass ICIE 16	–	2	379	3
[38]	2011	3-D printing	Bioactive glass (Si/Ca/P=80/15/5 M ratio)	60.4	16.10 ± 1.53	1307 ± 40, 1001 ± 48, 624 ± 40	7
[39]	2011	Replica (Polymer template)	Boron-based glasses	40–60	0.1–0.4	100–500	7
This study	2016	Powder Technology & Polymer Foaming	Bioglass 45S5	64–79	13.78 ± 2.43	25–600	7

low, compared with the value obtained in the present work, even those reported for scaffolds with less porosity, with the exception of the strengths reported by Wu et al. [38]. This compressive strength improvement in scaffolds prepared using mixed powder technology and the polymer foaming method may be associated with the consolidation of the struts within the structure of the foams, because the particles are better sintered as the sintering temperature increases [10]. This leads to a decrease in porosity between struts and particles, with the resulting increase in the mechanical properties of the structure. Forming a glass-ceramic by means of a sintering process results in crystallization and densification, the microstructure of the parent glass shrinks, porosity is reduced, and the solid structure gains mechanical strength. However, it has been confirmed that glass crystallization in Bioglass®-derived glass-ceramic scaffolds does not suppress bioactivity, it only retards the formation of the surface hydroxyapatite layer when the scaffold has been immersed in body fluid [18,25].

4. Conclusions

In conclusion, foams with 61.44 ± 3.13% porosity, sufficient to be a regenerative scaffold, were successfully sintered from a powder mixture of 45S5 bioactive glass, a polymeric binder, and a foaming agent. The porosity of the foams is open and interconnected with a pore size suitable for bone growth (25–600 μm). Primary ($Na_6Ca_3Si_6O_{18}$) and secondary ($Na_2Ca_4(PO_4)_2SiO_4$) crystalline phases were observed after sintering at 975 °C, as reported by other researchers. The compressive strength obtained is higher than that required for bone reconstruction applications, with an average of 13.78 ± 2.43 MPa.

Acknowledgments

The authors wish to thank the work group from the NRC-Industrial Materials Institute in Bourcherville, QC, Canada, for their technical support during the academic stay of Esmeralda Villicaña Molina. The present work was financially supported by the CONACYT under Grant No. CB-2013-C01-222262 and by the *Universidad Michoacana de San Nicolás de Hidalgo* (UMSNH) under Grant No. UMSNH-CIC-2014-2016-1.24 and the PIFI-PROFOCIE Program.

References

[1] M. Vallet-Regí, C.V. Ragel, A.J. Salinas, Glasses with medical applications, Eur. J. Inorg. Chem. 2003 (2003) 1029–1042.
[2] J.R. Jones, Reprint of: review of bioactive glass: from hench to hybrids, Acta Biomater. 23 (2015) S53–S82.
[3] D. Belluci, V. Cannillo, A. Sola, An overview of the effects of thermal processing on bioactive glasses, Sci. Sinter. 42 (2010) 307–320.
[4] A.R. Boccaccini, Q.Z. Chen, L. Lefebvre, L. Gremillard, J. Chevalier, Sintering, crystallisation and biodegradation behaviour of Bioglass-derived glass-ceramics, Faraday Discuss. 136 (2007) 27–44.
[5] J.R. Jones, E. Gentleman, J. Polak, Bioactive glass scaffolds for bone regeneration, Elements 3 (2007) 393–399.
[6] D. Bellucci, F. Chiellini, G. Ciardelli, M. Gazzarri, P. Gentile, A. Sola, V. Cannillo, Processing and characterization of innovative scaffolds for bone tissue engineering, J. Mater. Sci. Mater. Med. 23 (2012) 1397–1409.
[7] L.C. Gerhardt, A.R. Boccaccini, Bioactive glass and glass-ceramic scaffolds for bone tissue engineering, Materials 3 (2010) 3867–3910.
[8] S. Deb, R. Mandegaran, L. Di Silvio, A porous scaffold for bone tissue engineering/45S5 bioglass-derived porous scaffolds for co-culturing osteoblasts and endothelial cells, J. Mater. Sci.: Mater. Med. 21 (2010) 893–905.
[9] A.R. Studart, U.T. Gonzenbach, E. Tervoort, L.J. Gauckler, Processing routes to macroporous ceramics: a review, J. Am. Ceram. Soc. 89 (2006) 1771–1789.
[10] E.A. Aguilar-Reyes, C.A. Leon-Patino, B. Jacinto-Diaz, L.-P. Lefebvre, Structural characterization and mechanical evaluation of bioactive glass 45S5 foams obtained by a powder technology approach, J. Am. Ceram. Soc. 95 (2012) 3776–3780.
[11] T. Kokubo, H. Takadama, How useful is SBF in predicting in vivo bone bioactivity?, Biomaterials 27 (2006) 2907–2915.
[12] O. Bretcanu, X. Chatzistavrou, K. Paraskevopoulos, R. Conradt, I. Thompson, A.R. Boccaccini, Sintering and crystallization of 45S5 bioglass® powder, J. Eur. Ceram. Soc. 29 (2009) 3299–3306.
[13] V. Karageorgiou, D. Kaplan, Porosity of 3D biomaterial scaffolds and osteogenesis, Biomaterials 26 (2005) 5474–5491.

[14] P. Kasten, I. Beyen, P. Niemeyer, R. Luginbühl, M. Bohner, W. Richter, Porosity and pore size of β-tricalcium phosphate scaffold can influence protein production and osteogenic differentiation of human mesenchymal stem cells: an in vitro and in vivo study, Acta Biomater. 4 (2008) 1904–1915.
[15] L. Lefebvre, J. Chevalier, L. Gremillard, R. Zenati, G. Thollet, D. Bernache-Assolant, A. Govin, Structural transformations of bioactive glass 45S5 with thermal treatments, Acta Mater. 55 (2007) 3305–3313.
[16] D.C. Clupper, J.J. Mecholsky Jr., G.P. LaTorre, D.C. Greespan, Sintering temperature effects on the *in vitro* bioactive response of tape cast and sintered bioactive glass-ceramic in tris buffer, J. Biomed. Mater. Res. 57 (2001) 532–540.
[17] A. Sola, D. Bellucci, M.G. Raucci, S. Zappetelli, L. Ambrosio, V. Cannillo, Heat treatment of Na_2O-CaO-P_2O_5-SiO_2 bioactive glasses: densification processes and postsintering bioactivity, J. Biomed. Mater. Res. A 100A (2012) 305–322.
[18] O.P. Filho, G.P. La Torre, L.L. Hench, Effect of crystallization on apatite-layer formation of bioactive glass 45S5, J. Biomed. Mater. Res. 30 (1996) 509–514.
[19] M.H. Fathi, A. Hanifi, V. Mortazavi, Preparation and bioactivity evaluation of bone-like hydroxyapatite nanopowder, J. Mater. Process. Technol. 202 (2008) 536–542.
[20] M. Magallanes-Perdomo, S. Meille, J.-M. Chenal, E. Pacard, J. Chevalier, Bioactivity modulation of Bioglass® powder by thermal treatment, J. Eur. Ceram. Soc. 32 (2012) 2765–2775.
[21] J.R. Jones, L.L. Hench, Factors affecting the structure and properties of bioactive foam scaffolds for tissue engineering, J. Biomed. Mater. Res. B. Appl. Biomater. 68 (2004) 36–44.
[22] M.R. Filgueiras, G. La Torre, L.L. Hench, Solution effects on the surface reactions of three bioactive glass compositions, J. Biomed. Mater. Res. 27 (1993) 1485–1493.
[23] L.L. Hench, Bioceramics, J. Am. Ceram. Soc. 81 (1998) 1705–1728.
[24] D.U. Tulyaganov, M.E. Makhkamov, A. Urazbaev, A. Goel, J.M.F. Ferreira, Synthesis, processing and characterization of a bioactive glass composition for bone regeneration, Ceram. Int. 39 (2013) 2519–2526.
[25] Q.Z. Chen, I.D. Thompson, A.R. Boccaccini, 45S5 Bioglass®-derived glass-ceramic scaffolds for bone tissue engineering, Biomaterials 27 (2006) 2414–2425.
[26] S.B. Nicoll, Materials for bone graft substitutes and osseous tissue regeneration, in: J.A. Burdick, R.L. Mauck (Eds.), Biomaterials for Tissue Engineering Applications – A Review of Past and Future Trends, Springer, New York, 2011, pp. 343–362.
[27] P. Sepulveda, J.G. Binner, S.O. Rogero, O.Z. Higa, J.C. Bressiani, Production of porous hydroxyapatite by the gel-casting of foams and cytoxic evaluation, J. Biomed. Mater. Res. 50 (2000) 27–34.
[28] P. Sepulveda, J.R. Jones, L.L. Hench, Bioactive sol-gel foams for tissue repair, J. Biomed. Mater. Res. 59 (2002) 340–348.
[29] S. Callcut, J.C. Knowles, Correlation between structure and compressive strength in a reticulated glass-reinforced hydroxyapatite foam, J. Mater. Sci.: Mater. Med. 13 (2002) 485–489.
[30] P. Sepulveda, H.A. Bressiani, J.C. Bressiani, L. Meseguer, B. Konig Jr., In vivo evaluation of hydroxyapatite foams, J. Biomed. Mater. Res. 62 (2002) 587–592.
[31] H.R. Ramay, M. Zhang, Preparation of porous hydroxyapatite scaffolds by combination of the gel-casting and polymer sponge methods, Biomaterials 24 (2003) 3293–3302.
[32] H.R. Ramay, M. Zhang, Biphasic calcium phosphate nanocomposite scaffolds for load bearing bone tissue engineering, Biomaterials 25 (2004) 5171–5180.
[33] J.R. Jones, L.L. Hench, Factors affecting the structure and properties of bioactive foam scaffolds for tissue engineering, J. Biomed. Mater. Res. B 68B (2004) 36–44.
[34] X. Miao, G. Lim, K.-H. Loh, A.R. Boccaccini, Preparation and characterization of calcium phosphate bone cement, Mater. Proc. Prop. Perf. 3 (2004) 319–324.
[35] H.W. Kim, J.C. Knowles, H.E. Kim, Hydroxyapatite porous scaffold engineered with biological polymer hybrid coating for antibiotic vancomycin release, J. Mater. Sci.: Mater. Med. 16 (2005) 189–195.
[36] V. Cannillo, F. Chiellini, P. Fabbri, A. Sola, Production of bioglass 45S5-poly-caprolactone composite scaffolds via salt-leaching, Compos. Struct. 92 (2010) 1823–1832.
[37] Z.Y. Wu, R.G. Gill, S. Yue, D. Nightingale, P.D. Lee, J.R. Jones, Melt-derived bioactive glass scaffolds produced by a gel-cast foaming technique, Acta Biomater. 7 (2011) 1807–1816.
[38] C. Wu, Y. Luo, G. Cuniberti, Y. Xiao, M. Gelinsky, Three-dimensional printing of hierarchical and tough mesoporous bioactive glass scaffolds with a controllable pore architecture, excellent mechanical strength and mineralization ability, Acta Biomater. 7 (2011) 2644–2650.
[39] W. Liang, Y. Tu, H. Zhou, C. Liu, C. Rüssel, Borophosphate glass-ceramic scaffolds by a sodium silicate bonding process, J. Non-Cryst. Solids 257 (2011) 958–962.